



# Magneto-caloric effect in FeZrB amorphous alloys near room temperature

Pablo Álvarez<sup>a</sup>, Jorge Sánchez Marcos<sup>b</sup>, Pedro Gorria<sup>a,\*</sup>, Luis Fernández Barquín<sup>c</sup>, Jesús A. Blanco<sup>a</sup>

<sup>a</sup> Departamento de Física, Universidad de Oviedo, Avda. Calvo Sotelo, s/n, 33007 Oviedo, Spain

<sup>b</sup> Instituto de Ciencia de Materiales de Madrid, ICMM-CSIC, Cantoblanco, 28049 Madrid, Spain

<sup>c</sup> Departamento CITIMAC, Universidad de Cantabria, Avda. de los Castros, s/n, 39005 Santander, Spain

## ARTICLE INFO

### Article history:

Received 31 July 2009

Received in revised form 28 January 2010

Accepted 21 February 2010

Available online 3 March 2010

### Keywords:

Metallic glasses

Fe-based alloys

Magneto-caloric effect

## ABSTRACT

The magneto-caloric effect exhibited by three Fe-rich FeZrB amorphous alloys with different compositions and Curie temperatures between 230 and 300 K has been studied. Albeit the maximum entropy change is low ( $|\Delta S_M|^{\max} \sim 3 \text{ J kg}^{-1} \text{ K}^{-1}$  under an applied magnetic field change from 0 to 50 kOe), the magneto-caloric effect (MCE) spreads out over a broad temperature interval ( $\Delta T \sim 200 \text{ K}$ ). The estimated values for the relative cooling power are close to that of pure Gd. From the applied magnetic field dependence of the magnetic entropy change a master curve valid for these Fe-rich FeZrB amorphous alloys has been found. However, two reference temperatures of the  $|\Delta S_M|(T)$  are needed in order to get a collapsing curve for all the maximum applied magnetic field values. The latter suggests that the striking magnetic behaviour of these compounds below 200 K influences the MCE effect. Moreover, the collapse into the same curve for different rescaled temperature dependences of the magnetic entropy change in the three samples implies the existence of similar magnetic interactions in these compounds.

© 2010 Elsevier B.V. All rights reserved.

## 1. Introduction

The most challenging purpose for refrigeration technology is the optimization of the engine efficiency minimizing both the powder consumption as well as the environmental impact. The emerging technology based on magnetic refrigeration will probably be the most adequate way to fulfill these requirements [1–3]. Therefore, the search for new materials displaying significant magneto-caloric effect (MCE) is nowadays a very active field of research [4–8]. For applications near room temperature (where the temperature difference between the hot and cold reservoirs for a domestic refrigerator could be higher than 80 K), rather than a material with high or giant magnetic entropy change,  $|\Delta S_M|$ , inside a narrow temperature interval (as occurring around a first-order phase transition) [1,2], it is needed a broad  $|\Delta S_M|(T)$  peak expanded over the temperature range where the refrigerant engine should operate. Some ferromagnetic materials exhibit moderate MCE over wide temperature ranges around their second-order (ferro-to-paramagnetic) phase transition (SOPT), such as it is the case of pure Gd [1], rare-earth intermetallic compounds [1,2,6–8] or some manganites [9]. Recently, disordered and non-crystalline magnetic materials displaying SOPT such as rare-earth-based amorphous ribbons [10,11] and bulk metallic glasses [12,13], ball milled amorphous alloys [14,15], as well as Fe-rich metallic glasses [16,17] have attracted

emergent relevance in the field. The reason for that is the broad  $|\Delta S_M|(T)$  peak exhibited, being even larger than 150 K under applied magnetic field changes of 50 kOe, although the maximum of  $|\Delta S_M|$  is relatively low compared to that of other materials displaying MCE.

In the case of Fe-rich metallic glasses, the MCE is due to Fe atoms, and they present several advantages that must be pointed out, namely, (i) lower fabrication costs due the absence of rare-earth metals in the composition, (ii) the ultra-soft magnetic properties, with vanishing magnetocrystalline anisotropy and very low coercive fields, withdraw any energy losses due to hysteresis effects thus allowing higher operation frequencies and faster response, and (iii) the magnetic transition temperatures, and then the temperature ranges for the MCE, can be easily adjustable by selecting the appropriate composition. Upto now, the most studied compositions consist of around 70–80 at.% of Fe with upto 15–20 at.% of metalloid elements (B, Si, P, Ge, ...) and small amounts of one or more transition metal atoms (Nb, Mo, Co, Cr, Zr, Mn, ...) [18–22]. However, in almost all the cases the Curie temperatures,  $T_C$ , are above room temperature, therefore if the material should be used in a refrigerant engine for cooling from room to lower temperatures, the maximum of the MCE must occur just below room temperature. In this way, FeZrB metallic glasses are good candidates for fulfilling the latter requirements, since these alloys combine high values for the saturation magnetization (above  $1.5 \mu_B/\text{Fe at.}$ ) with  $T_C$  values above 200 K.

Fe-rich FeZr metallic glasses are ferromagnetic below room temperature and possess crystallization temperatures above 750 K

\* Corresponding author. Tel.: +34 985102899; fax: +34 985103324.

E-mail address: [pgorria@uniovi.es](mailto:pgorria@uniovi.es) (P. Gorria).

[23]. These alloys display striking magnetic behaviours including re-entrant spin-glass, exceptional magneto-volume effects and a reduction of  $T_C$  with increasing Fe content, due to the strong competition between Fe–Fe magnetic interactions [24–26]. The addition of boron upto 10 wt%. gives rise to a large increase in  $T_C$  (upto around 400K), without losing complexity in the magnetic behaviour [27,28]. Moreover, these alloys have attracted huge attention because after adequate heat treatments a stable nanocrystalline microstructure is reached, thus displaying ultra-soft magnetic properties [29] and allowing the study of magnetic interactions between the Fe nanocrystals and the remaining amorphous matrix [30,31]. In this article we show that although FeZrB amorphous alloys do not exhibit large MCE values, the estimated relative cooling power (RCP) or refrigerant capacity (RC) values are comparable with those of other reference materials such is the case of pure gadolinium. In addition, the dependencies of  $|\Delta S_M|$  with both the temperature and the applied magnetic field have been studied in terms of a master curve via renormalization of temperature scale.

**2. Experimental details and data analysis**

The amorphous ribbons of compositions  $Fe_{91}Zr_7B_2$  (B2),  $Fe_{88}Zr_8B_4$  (B4) and  $Fe_{87}Zr_6B_6Cu_1$  (B6) with  $1.5\text{ mm} \times 20\text{ }\mu\text{m}$  cross-sections were fabricated by melt-spinning under Ar atmosphere from the arc-melted master alloys. The absence of intense peaks in the X-ray diffraction patterns, in which only broad haloes are present, confirms the amorphous state of the ribbons. Around 40 isothermal magnetization vs applied magnetic field,  $M(H)$  curves, were measured using a SQUID magnetometer in the temperature range between 50 and 370 K (see Fig. 1 right bottom panel for several  $M(H)$  curves corresponding to B6 sample). The temperature steps between consecutive isothermal  $M(H)$  curves were 4 K in the immediacy of the Curie temperature (between  $T_C - 30\text{ K}$  and  $T_C + 30\text{ K}$ ) and 10 K out of this temperature region. At each temperature the data were collected under constant  $dc$  applied magnetic field steps of  $H = 1\text{ kOe}$  in the magnetic field range between 0 and 50 kOe.

The MCE as a function of the applied magnetic field and the temperature has been obtained from the magnetic entropy change,  $\Delta S_M$ , taking into account that for an isothermal process,  $\Delta S_M$  can be evaluated integrating the adequate Maxwell relation [32]:

$$\Delta S_M(H, T) = S_M(H, T) - S_M(0, T) = \int_0^H \left( \frac{\partial M}{\partial T} \right)_H dH \quad (1)$$

Note that at a fixed temperature  $T$ , the magnetic entropy under an applied magnetic field  $H$  and in the absence of the magnetic field are  $S_M(H, T)$  and  $S_M(0, T)$ , respectively.

Essentially, the value for  $\Delta S_M$  at a given temperature is obtained after a numerical integration of two consecutive  $M(H)$  isotherms around such temperature, followed by the numerical derivative with temperature. The results obtained after applying this procedure to the whole set of  $M(H)$  measured curves allow us to obtain the temperature and/or applied magnetic field dependences of the magnetic entropy,  $|\Delta S_M|(H, T)$ .

For applications in magnetic refrigeration at room temperature is important to take into account the amount of heat that the studied material can absorb during the refrigeration cycle from the cold focus. For that reason the most common parameter used to quantify this are either RCP or RC, that can be defined in several ways [6,32]; in this paper we have chosen the product of the maximum  $|\Delta S_M|$  peak value and the full width at half maximum,  $\delta T_{FWHM}$ ,

$$RCP(S) = |\Delta S_M|^{\max} \times \delta T_{FWHM} \quad (2)$$

The magnetic field dependence of  $|\Delta S_M|$  is analytically calculated using the following expression:

$$n = \frac{d |\ln(\Delta S_M)|}{d \ln T} \quad (3)$$

In a material with second-order transition, the  $\Delta S_M(T)$  curves for different maximum magnetic fields collapse into a single master curve [20]. That master curve is useful for predicting the field dependence of the magnetic entropy change and extrapolating it over both the experimental temperature and magnetic field range available in a laboratory. The master curve is obtained as follow: first, the  $\Delta S_M(T)$  curves are normalized to its maximum value  $\Delta S_M^{\text{Peak}}$  for each maximum applied magnetic field, and then, if there is no presence of a secondary magnetic phase, the temperature axis is rescaled as [33]:

$$\theta = \frac{(T - T_r)}{(T_r - T_C)} \quad (4)$$

where  $T_r$  is a reference point in the curve corresponding to a certain fraction of  $\Delta S_M^{\text{Peak}}$ . If another magnetic phase exists or the material exhibits magnetic inhomogeneities is necessary the use of two different reference temperatures, which leads to:

$$\theta = - \frac{(T - T_C)}{(T_{r1} - T_C)} \quad T < T_C \quad (5)$$

$$\theta = \frac{(T - T_C)}{(T_{r2} - T_C)} \quad T > T_C \quad (6)$$

where  $T_{r1}$  and  $T_{r2}$  are the temperatures of the two reference points of each curve that correspond to a  $\Delta S_M^{\text{Peak}}$ , with  $a$  in between 0 and 1.

**3. Results and discussion**

In Fig. 1 the temperature dependence of the  $|\Delta S(H)|$  curves for the  $Fe_{91}Zr_7B_2$  (B2),  $Fe_{88}Zr_8B_4$  (B4) and  $Fe_{87}Zr_6B_6Cu_1$  (B6) studied

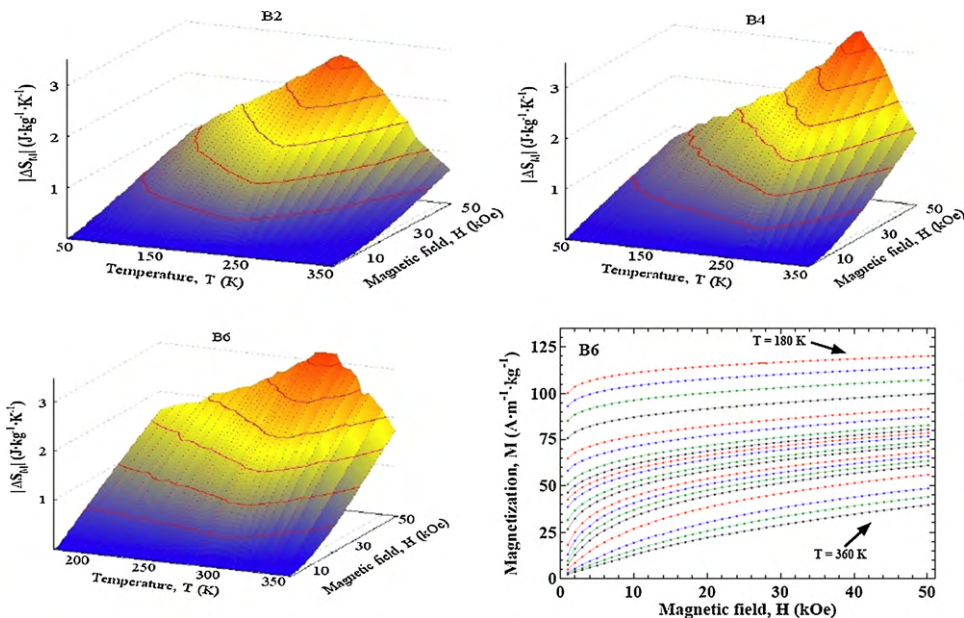


**Fig. 1.** Temperature and applied magnetic field dependencies of the magnetic entropy change,  $|\Delta S_M|$ , for B2, B4 and B6 samples. Right bottom panel displays some of the measured  $M(H)$  isotherms for the B6 sample from which  $|\Delta S_M|(T, H)$  surfaces have been obtained (see text).

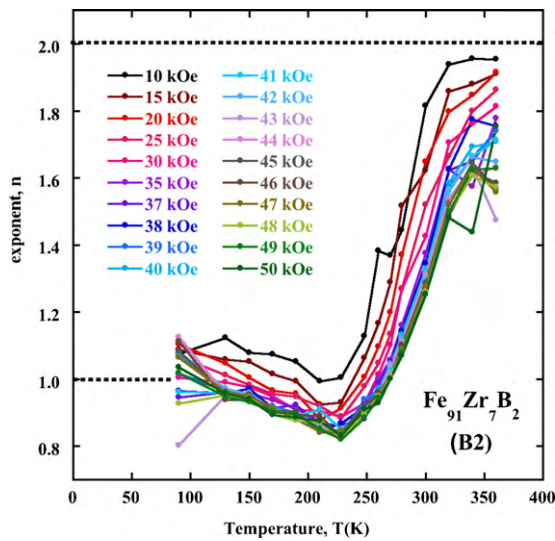


**Fig. 2.** Temperature dependence of the exponent of the magnetic entropy change under different applied magnetic field values for  $\text{Fe}_{91}\text{Zr}_7\text{B}_2$ . Lines are guides for the eyes. The dashed lines correspond to the paramagnetic  $n=2$  value and the low temperature (far from  $T_C$ ) ferromagnetic  $n=1$  value.

samples are shown. The maximum  $|\Delta S_M|$  values for an applied magnetic field change from 0 to 50 kOe are 2.8, 3.3 and 3.2  $\text{J kg}^{-1} \text{K}^{-1}$  for B2, B4 and B6 alloys, respectively. Those values correspond approximately to a quarter of the value for pure gadolinium under the same applied magnetic field change. The temperatures of the  $|\Delta S_M|(T)$  peaks are around 250 (B2), 295 (B4) and 300 K (B6). The RCP values calculated as mentioned in the previous section, are 532 (B2), 649 (B4) and 577  $\text{J kg}^{-1}$  (B6), which are around 80–90% of the value for pure Gd. This fact is due to a large temperature span of the  $|\Delta S_M|(T)$  peak, which could reach  $\delta T_{\text{FWHM}} \approx 150\text{--}200$  K. While the maximum values of  $|\Delta S_M|$  are similar in B4 and B6 samples and higher than that calculated for B2, the  $|\Delta S_M|(T)$  peak is broader (larger  $\delta T_{\text{FWHM}}$ ) for B2 than for B4 and B6. These two features are closely related to a higher magnetic moment for the Fe atoms in both B4 and B6 ( $\mu \approx 1.6 \mu_B$ ) respect to B2 sample ( $\mu \approx 1.4 \mu_B$ ), and the slower drop of the magnetization with temperature of the B2 samples in de immediacy of  $T_C$  [34]. It is worth noting that in addition to both  $\Delta S(H)$  and RCP values, also the temperature range in which the MCE occurs is important for practical applications. As it is well known, the maximum of the magnetic entropy change of a ferromagnetic material is achieved close to its Curie temperature,  $T_C$ . Hence, for refrigeration purposes at room temperature it is important the feasible control of the  $T_C$  value of the material via slight compositional changes. This requirement is fulfilled by FeZrB(Cu) metallic glasses, because  $T_C$  follows an almost linear dependence with the Fe atomic percentage (with a negative slope), being nearly independent of the relative amount of Zr and B [27,30,34]. Therefore, the temperature range for the refrigeration cycle can be tuned between 100 and 350 K.

On the other hand, the value of the magnetic entropy change depends on the measuring temperature, but also on the maximum magnetic field change. Then, for a material displaying a second-order ferromagnetic transition, it can be expected that such dependencies for each temperature follow a potential law,  $\Delta S_M \propto H^n$  [17]. We show in Fig. 2 the variation of the exponent  $n$  with temperature for different maximum magnetic field changes (from  $\Delta H = 10$  kOe to  $\Delta H = 50$  kOe).

The  $n$  values at each temperature have been obtained through the fit of the  $|\Delta S_M|(H)$  curves using Eq. (3). As it can be observed,  $n$  depends on the magnetic state of the compound. While  $n \approx 2$

for temperatures well above  $T_C$ , being a direct consequence of the Curie–Weiss law [35], its value goes to 1 in ferromagnetic state far enough from  $T_C$ . Moreover,  $n(T)$  curves display a minimum at  $T \approx T_C$  (see Fig. 2).

In the framework of the mean field theory (MFT), a minimum for the exponent  $n$  at  $T = T_C$  with a constant value of  $n = 2/3$  and being independent of the applied magnetic field is expected. In addition,  $n$  can be related to the critical exponents  $\beta$  and  $\gamma$  at the magnetic phase transition in the following way:

$$n = 1 + \frac{\beta - 1}{\beta + \gamma} \quad (7)$$

where  $\beta = 0.5$  and  $\gamma = 1$  in MFT. However, in FeZrB amorphous alloys  $n$  exhibits a clear dependence on the applied magnetic field, with diminishing values down to  $n \approx 0.82$  for  $H \geq 45$  kOe, as  $H$  is increased in B2 sample. The origin of this  $n(H)$  dependence can be attributed to the fact that  $\text{Fe}_{91}\text{Zr}_7\text{B}_2$  amorphous alloy is far from being magnetically saturated under an applied magnetic field  $H = 10$  kOe, due to the complex competing magnetic interactions between Fe atoms [27,34]. For  $H > 10$  kOe the  $M(H)$  curve reduces gradually its slope, thus explaining the almost constant value of  $n$  for  $H \geq 45$  kOe (see Fig. 2).

Although similar behaviour is observed for B4 and B6 samples, the  $H$ -dependence of  $n$  (not shown) is less pronounced because these compounds are closer to be magnetically saturated. Concerning the minimum values of  $n$  for these B4 and B6 samples,  $n \approx 0.77$  in both cases under an applied magnetic field change from 0 to 50 kOe. Therefore, it can be concluded that the mean field model no longer applies to these compounds. Moreover, the change in the value of the exponent  $n$  as the boron content increases can be correlated with the magnetic state of the samples, and in particular with the compositional dependence of the exponent  $n$ , as follows. If the exponent  $\beta$  is estimated from the high field  $M(H)$  curves by means of modified Arrott plots [ $M^{1/\beta}$  vs  $(H/M)^{1/\gamma}$ ], using a value of  $\gamma = 1.38$  [34],  $\beta$  varies from 0.325 in B2 sample to 0.39 and 0.4 in B4 and B6 samples, respectively.  $\beta$  values lower than 0.5 indicate the existence of magnetic inhomogeneities in a ferromagnetic compound [36,37]. Hence, the compounds became magnetically more homogeneous as the boron content increases [34], thus exhibiting smaller and nearly magnetic field independent minimum values of the  $n$  exponents, as is the case of B4 and B6 alloys in comparison with B2 one.

As a consequence of the low temperature re-entrant spin-glass behaviour exhibited by these FeZrB compounds, already attributed to the existence of ferromagnetic clusters inside a ferromagnetic matrix with different spin dynamics and competing interactions [26,28], Eq. (2) lose its validity. On the other hand, Franco et al. proposed that the magnetic field dependence of  $n$  is due to the contribution coming from a second magnetic phase [33]. In our case, the  $n(H)$  dependence cannot be attributed to any secondary magnetic phase, even though the effects are the same, with the difference that above certain applied magnetic field ( $H \geq 45$  kOe for B2)  $n$  is almost constant.

With the aim of getting a more detailed knowledge of the temperature dependence of the magnetic entropy change in these alloys, we have normalized the  $|\Delta S_M(T)|$  curves and rescaled the temperature axis in order to show if these curves collapse into a single master curve for different values of the applied magnetic field. In the case of B2 sample two different reference temperatures [see Eqs. (5) and (6)] are needed as it can be seen in Fig. 3 where the curves for  $H \geq 20$  kOe scale into a master curve in the entire temperature range, which indicates that no other magnetic transition can be expected in the temperature interval of the measurements [35]. The use of only one reference temperature gives rise to non-collapsing curves in the low temperature range (not shown), being a clear signature of the magnetic inhomogeneous

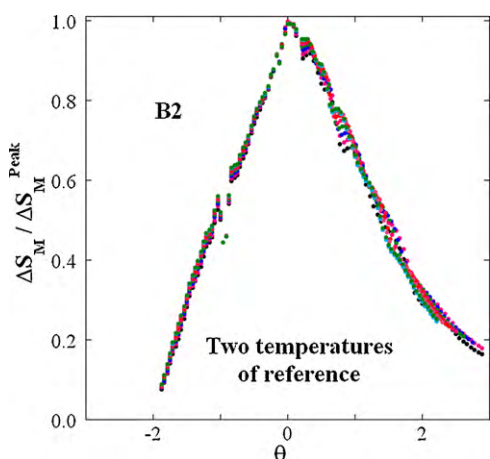


**Fig. 3.** Master curve of the magnetic entropy change for the  $\text{Fe}_{91}\text{Zr}_7\text{B}_2$  amorphous alloy determined from different maximum applied fields, ranging from 20 to 50 kOe and using two reference temperatures.

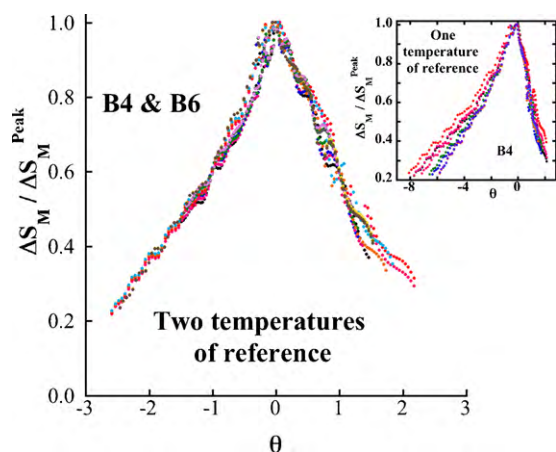


**Fig. 4.** Collapse into the same master curve of the rescaled temperature dependence of magnetic entropy change of  $\text{Fe}_{88}\text{Zr}_8\text{B}_4$  and  $\text{Fe}_{87}\text{Zr}_6\text{B}_6\text{Cu}_1$  obtained using two temperatures of reference.

state of the alloy, which exhibits re-entrant spin-glass behaviour below 100 K [26,28].

A similar trend is followed by B4 and B6 samples as it can be observed in Fig. 4, where two reference temperatures have been also considered. It is worth noting that the curves for both samples collapse into the same master curve, thus confirming a similar magnetic behaviour of these two compounds (we must remember that the values for  $T_C$ ,  $\beta$  and  $n$  exponents are close in B4 and B6 amorphous alloys). The inset of Fig. 4 shows the normalized curve of the magnetic entropy change for several applied magnetic fields of B4 sample, when only one reference temperature is used. Obviously the different curves do not collapse into a single master curve in the low temperature range.

Taking into account that almost an identical curve is obtained for B6 sample, a similar inhomogeneous magnetic state could be expected for both B4 and B6 alloys at low temperature, as it was already probe by SQUID magnetometry and Mössbauer spectroscopy [34].

#### 4. Summary and conclusions

We have studied the magneto-caloric effect on three FeZrB amorphous ribbons with different boron content and Curie temperatures ranging from 230 to 300 K. The maximum magnetic entropy change of the ribbons are low when compared with

Gd-based alloys, but they exhibit a broad  $|\Delta S_M(T)|$  peaks extending over 150–200 K under applied magnetic field changes from 0 to 50 kOe. The latter gives rise to elevated values for the relative cooling power or refrigerant capacity, which can be comparable to that of pure gadolinium. The applicability of these alloys in real refrigeration engines is today a matter of controversy. However, we have tried to find a relationship between the temperature and applied magnetic field dependencies of the magnetic entropy change with the complex and inhomogeneous magnetic state of these alloys. In order to get a single master curve resulting from a collapse of the normalized magnetic entropy curves, we have shown that two different temperatures of reference are needed instead of using only one reference temperature, like in conventional ferromagnetic alloys. The magnetic inhomogeneous state of these alloys, due to competing magnetic interactions between Fe atoms, is the most plausible scenario for explaining the magnetic behaviour in these Fe-rich FeZrB amorphous alloys including the magnetic field and temperature dependencies of the magneto-caloric effect.

#### Acknowledgements

Financial support from FEDER and the Spanish MICINN (NAN2004-09203-C04 and MAT2008-06542-C04) is acknowledged. Two of us (PA and JSM) thank FICYT and MICINN for PhD and “Juan de la Cierva” research contracts, respectively.

#### References

- [1] A.M. Tishin, Y.I. Spichkin, The Magnetocaloric Effect and its Applications, IOP Publishing, Bristol, 2003.
- [2] K.A. Gschneidner Jr., V.K. Pecharsky, A.O. Tsokol, Rep. Prog. Phys. 68 (2005) 1479.
- [3] E. Brück, J. Phys. D: Appl. Phys. 38 (2005) R381.
- [4] O. Tegus, E. Brück, K.H.J. Buschow, F.R. de Boer, Nature (Lond.) 415 (2002) 150.
- [5] J. Lyubina, K. Nenkov, L. Schultz, O. Gutfleisch, Phys. Rev. Lett. 101 (2008) 177203.
- [6] P. Gorria, J.L. Sánchez Llamazares, P. Álvarez, J. Sánchez Marcos, M.J. Pérez, J.A. Blanco, J. Phys. D: Appl. Phys. 41 (2008) 192003.
- [7] Q. Zhang, J.H. Cho, J. Du, F. Yang, X.G. Liu, W.J. Feng, Y.J. Zhang, J. Li, Z.D. Zhang, Solid State Commun. 149 (2009) 396.
- [8] P. Gorria, P. Álvarez, J. Sánchez Marcos, J.L. Sánchez Llamazares, M.J. Pérez, J.A. Blanco, Acta Mater. 57 (2009) 1724.
- [9] M.-H. Phan, S.-C. Chu, J. Magn. Magn. Mater. 308 (2007) 325.
- [10] S. Tencé, S. Gorsse, E. Gaudin, B. Chevalier, Intermetallics 17 (2009) 115.
- [11] Q.Y. Dong, B.G. Shen, J. Chen, J. Shen, F. Wang, H.W. Zhang, J.R. Sun, Solid. State Commun. 149 (2009) 417.
- [12] L. Liang, X. Hui, C.M. Zhang, G.L. Chen, J. Alloys Compd. 463 (2008) 30.
- [13] J. Du, Q. Zheng, E. Brück, K.H.J. Buschow, W.B. Cui, W.J. Feng, Z.D. Zhang, J. Magn. Magn. Mater. 321 (2009) 413.
- [14] B. Chevalier, J.-L. Bobet, J. Sánchez Marcos, J. Rodríguez Fernández, J.C. Gómez Sal, Appl. Phys. A 80 (2005) 601.
- [15] J.J. Ipus, J.S. Blázquez, V. Franco, A. Conde, L.F. Kiss, J. Appl. Phys. 105 (2009) 123922.
- [16] V. Franco, J.S. Blázquez, C.F. Conde, A. Conde, Appl. Phys. 88 (2006) 042505.
- [17] V. Franco, J.S. Blázquez, A. Conde, J. Appl. Phys. 100 (2006) 064307.
- [18] I. Skorvanek, J. Kovac, Czech. J. Phys. 54 (2004) D189.
- [19] F. Johnson, R.D. Shull, J. Appl. Phys. 99 (2006) 08K909.
- [20] V. Franco, J.S. Blázquez, A. Conde, Appl. Phys. Lett. 89 (2006) 222512.
- [21] V. Franco, A. Conde, L.F. Kiss, J. Appl. Phys. 104 (2008) 033903.
- [22] Y.K. Fang, C.C. Yeh, C.C. Hsieh, C.W. Chang, H.W. Chang, W.C. Chang, X.M. Li, W. Li, J. Appl. Phys. 105 (2009) 07A910.
- [23] P. Gorria, J.S. Garitaonandia, M.J. Pérez, J.A. Blanco, J. Campo, Phys. Status Solidi (RRL) 3 (2009) 28.
- [24] S.N. Kaul, Phys. Rev. B 27 (1983) 6923.
- [25] J.M. Barandiarán, P. Gorria, I. Orue, M.L. Fdez-Gubieda, F. Plazaola, A. Hernando, Phys. Rev. B 54 (1996) 3026.
- [26] R. García Calderón, L. Fernández Barquín, S.N. Kaul, J.C. Gómez Sal, P. Gorria, J.S. Pedersen, R.K. Heenan, Phys. Rev. B 71 (2005) 134413.
- [27] J.M. Barandiarán, P. Gorria, J.C. Gómez Sal, L. Fernández Barquín, S.N. Kaul, IEEE Trans. Mag. 30 (1994) 4776.
- [28] L. Fernández Barquín, J.C. Gómez Sal, P. Gorria, J.S. Garitaonandia, J.M. Barandiarán, Eur. Phys. J. B 35 (2003) 3.
- [29] P. Gorria, I. Orue, F. Plazaola, M.L. Fernández-Gubieda, J.M. Barandiarán, IEEE Trans. Mag. 29 (1993) 2682.

- [30] A. Slawska-Waniewska, P. Nowicki, H.K. Lachowicz, P. Gorria, J.M. Barandiarán, A. Hernando, *Phys. Rev. B* 50 (1994) 6465.
- [31] J.S. Garitaonandia, P. Gorria, L. Fernández Barquín, J.M. Barandiarán, *Phys. Rev. B* 61 (2000) 6150.
- [32] V.K. Pecharsky, K.A. Gschneidner Jr., *J. Appl. Phys.* 90 (2001) 4614.
- [33] V. Franco, R. Caballero-Flores, A. Conde, Q.Y. Dong, H.W. Zhang, *J. Magn. Magn. Mater.* 321 (2009) 1115.
- [34] J.M. Barandiarán, P. Gorria, I. Orúe, M.L. Fernández-Gubieda, F. Plazaola, J.C. Gómez Sal, L. Fernández Barquín, L. Fournes, *J. Phys. : Condens. Matter.* 9 (1997) 5671.
- [35] V. Franco, A. Conde, V.K. Pecharsky, K.A. Gschneidner Jr., *EPL* 79 (2007) 47009.
- [36] A. Aharoni, *J. Appl. Phys.* 56 (1984) 3479.
- [37] A. Aharoni, *J. Appl. Phys.* 57 (1985) 648.